Inner Field Compensation as a Tool for the Characterization of Asymmetric Membranes and Peptide-Membrane Interactions

Sven O. Hagge, Andre Wiese, Ulrich Seydel, and Thomas Gutsmann
Research Center Borstel, Leibniz Center for Medicine and Biosciences, Department of Immunochemistry and Biochemical Microbiology, Division of Biophysics, D-23845 Borstel, Germany

ABSTRACT   Symmetric and asymmetric planar lipid bilayers prepared according to the Montal-Mueller method are a powerful tool to characterize peptide-membrane interactions. Several electrical properties of lipid bilayers such as membrane current, membrane capacitance, and the inner membrane potential differences and their changes can be deduced. The time-resolved determination of peptide-induced changes in membrane capacitance and inner membrane potential difference are of high importance for the characterization of peptide-membrane interactions. Intercalation and accumulation of peptides lead to changes in membrane capacitance, and membrane interaction of charged peptides induces changes in the charge distribution within the membrane and with that to changes in the membrane potential profile. In this study, we establish time-resolved measurements of the capacitance minimization potential $\Delta\Psi$ on various asymmetric planar lipid bilayers using the inner field compensation method. The results are compared to the respective ones of inner membrane potential differences $\Delta\Phi$ determined from ion carrier transport measurements. Finally, the time courses of membrane capacitances and of $\Delta\Psi$ have been used to characterize the interaction of cathelicidins with reconstituted lipid matrices of various Gram-negative bacteria.

INTRODUCTION

Membranes form the outer boundary of living cells or of internal cell compartments. Biological membranes have a dual function: i), they separate vital but incompatible metabolic processes conducted in the organelles and protect the cell against toxic processes; and ii), they maintain steady state of fluxes of specific ions, nutrients, wastes, and metabolic products in organelles and cells and, to provide this, they allow specific permeation of these products. Membranes consist largely of lipid bilayers composed of phospholipids, cholesterol, and/or glycolipid molecules. Embedded in or associated to this lipid matrix are the proteins, which have divers function for the survival of the cell.

A powerful tool to investigate interactions between membranes and peptides are symmetric and asymmetric planar lipid bilayers prepared according to the Montal-Mueller method (1972). These membranes can be used to perform electrical measurements for the investigation of pore formation induced by antimicrobial peptides or membrane proteins. In the case of pore-forming peptides, from the time-resolved determination of membrane current, the size and the lifetime of membrane lesions and their current voltage (I/U) characteristics can be deduced. In those cases, in which the accumulation of the peptide at the membrane surface or the intercalation into the lipid matrix does not lead to membrane permeabilization— either in the initial phase of peptide-membrane interaction or for nonpore-forming peptides—other membrane properties such as membrane capacitance and inner membrane

potential difference can be used to characterize the interaction process.

The membrane capacitance yields information about area, thickness, and composition of the lipid bilayer (Gutsmann et al., 2001). The accumulation of peptides on the bilayer surface or their intercalation into the lipid bilayer causes changes of these parameters and with that of membrane capacitance. The interaction with charged molecules such as polycationic antimicrobial peptides may also lead to changes in the electrostatic potential profile across the bilayer (Schoch et al., 1979). The three main contributions to the intrinsic membrane potential (Fig. 1) arise from i), the charged groups of lipid molecules (as phosphate, carboxylate, amino groups) expressed at the membrane surface and generating a surface potential, which—according to Gouy and Chapman (for review see (Cevc, 1990))—decreases exponentially within a distance of a few nanometers from the membrane surface (Gouy-Chapman potential V_G); ii) the dipole potential (V_D) inside the lipid bilayer caused by oriented dipoles of bound water molecules (Zheng and Vanderkooi, 1992); and iii), the Born self-energy (Born potential, V_B), which is the energy necessary to transfer a charge from a medium with a high dielectric constant ε (water) to one with a low ε (membrane) (Schoch et al., 1979). V_B is smoothed near the interface by interaction with induced dipoles (Neumcke and Läuger, 1969; Parsegian, 1975). Differences of the potentials between the two bilayer leaflets composed of different lipids lead to an inner membrane potential difference.

There are two common methods for the determination of the inner membrane potential difference. A procedure introduced by Schoch and co-workers (Schoch et al., 1979) is based on the ion carrier-mediated membrane permeability. Under the assumption of a trapezoidal potential profile (Fig. 1 A), the potential difference $\Delta\Phi$ between the two corners is given by
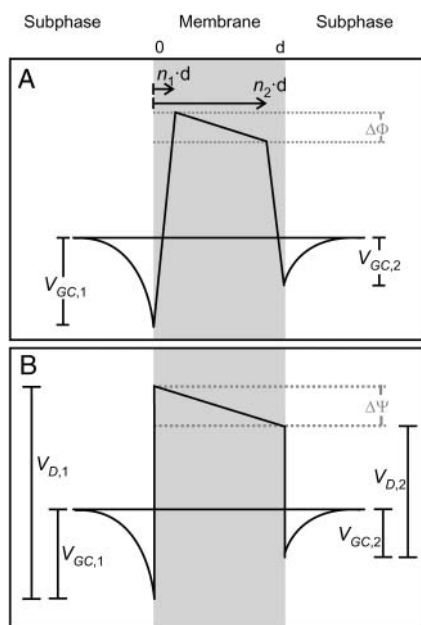
FIGURE 1 Potential profile across an asymmetric bilayer membrane (adopted from Schoch et al. (1979)).

$$\Delta\Phi = \Delta V_B(n_1, n_2) + (n_2 - n_1)(\Delta V_G + \Delta V_D) \qquad (1)$$

and can be determined from the I/U characteristics of carrier-doped membranes by curve fitting (Schoch et al., 1979; Seydel et al., 1992). This method has, however, two major drawbacks: i), the bilayer system has to be doped with a carrier molecule, which might influence the measurement and ii), a time-resolved measurement of $\Delta\Phi$ is not possible because the recording of a I/U curve takes several minutes.

These disadvantages can be overcome by applying the inner field compensation (IFC) method (Sokolov and Kuz'min, 1980). It is known that membrane capacitance is a function of the effective potential (Babakov et al., 1966; White, 1970). This potential, is composed of two components, the externally applied voltage U and the intrinsic potential $\Delta\Psi$, which is due to differences in the surface potentials V_G and V_D on the two sides of the bilayer (Fig. 1 B)

$$\Delta\Psi = \Delta V_G + \Delta V_D. \qquad (2)$$

The membrane capacitance as a function of the applied voltage is given by

$$C_M = C_0(1 + \alpha(\Delta\Psi + U)^2) \qquad (3)$$

(Fig. 3 A), where C_0 is the minimal capacitance (Schoch and Sargent, 1976) and α is a constant for each individual membrane. For planar bilayers according to Montal and Mueller, α was found to be ~ 0.02 V^{-2} (Alvarez and Latorre, 1978). Therefore, C_M adopts its minimum, when the intrinsic potential $\Delta\Psi$ is compensated by the externally applied potential U. Thus, $\Delta\Psi$ is also called capacitance minimiza-

tion potential. Experimentally, the bilayer is excited with a voltage composed of a dc and a sinusoidal contribution yielding a capacitive current response at the second harmonic of the stimulus, which vanishes at $U = -\Delta\Psi$ (Fig. 3, B and C) (Carius, 1976; Pohl et al., 2000, 1997, 1998).

Interaction of membrane active peptides with lipid bilayers may induce changes of membrane properties such as conductance, capacitance, and the two inner membrane potentials. In times of rising bacterial resistances against common antibacterial peptides, it becomes more and more important to get a deep understanding of the underlying processes of membrane permeabilization induced by the peptides. In bilayer reconstitution systems of bacterial lipid membranes, we used the four parameters to characterize the interaction mechanisms between peptides and bacterial membranes.

The cell envelope of Gram-negative bacteria consists of the cytoplasmic membrane, the peptidoglycan layer, and an additional barrier, the outer membrane (OM), which is strictly asymmetric with respect to its lipid composition (Lugtenberg and Van Alphen, 1983). Whereas the inner membrane is composed on both sides of phospholipids, the OM consists of a phospholipid inner leaflet and a lipopolysaccharide (LPS) outer leaflet. LPS consists of an oligo- or polysaccharide portion covalently linked to a lipid component, termed lipid A, which anchors the molecule in the membrane (Rietschel et al., 1994). In wild-type strains, the polysaccharide portion consists of an O-specific chain and the core oligosaccharide. Rough mutant strains do not express the O-specific chain, but retain core oligosaccharides of varying length. Deep-rough mutant LPS (Re LPS) represents the minimal structure of LPS consisting of only lipid A and two 3-deoxy-D-*manno*-oct-2-ulosonic acid (Kdo) monosaccharides (Holst, 1999) (Fig. 2).

For asymmetric LPS/phospholipid bilayers resembling the lipid matrix of the OM of Gram-negative bacteria, an extreme asymmetry in charge densities as well as in headgroup conformations occurs at neutral pH. Of the phospholipids of the inner leaflet of the OM, only the phosphatidylglycerol molecule, which makes up $\sim 20\%$ of the total phospholipids, carries one negative charge, whereas each LPS molecule (outer leaflet) carries at least 3–4 negative charges. The resulting surface charge densities are -3.25 e_0/nm^2 for Re LPS from *Escherichia coli* strain F515 (LPS F515) and -0.31 e_0/nm^2 for the phospholipid mixture (PL)—resembling the inner leaflet of the OM, respectively, since the molecular cross section of an LPS F515 molecule is 1.23 nm^2 and that of a diacyl phospholipid is 0.55 nm^2 (determined from monolayer isotherms with a film balance).

These negative charges at the LPS molecules (Fig. 2) induce a negative surface potential at the outer leaflet of the OM, which leads to an up-concentration of polycationic antimicrobial peptides, such as polymyxin B (Schindler and Teuber, 1975; Wiese et al., 1998; Kubesch et al., 1987;
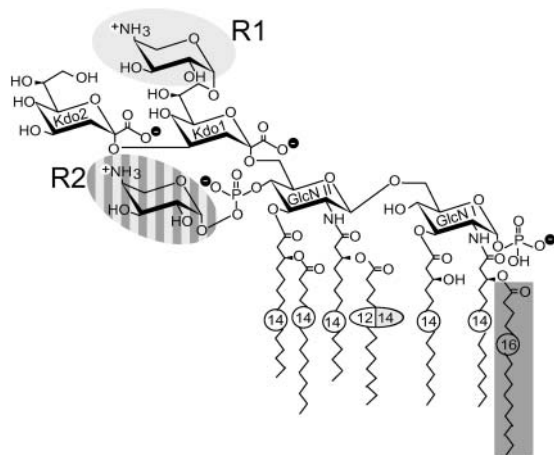
	LPS F515	LPS R595	LPS R45
R1	0 %	65 %	50 %
R2	0 %	0 %	50 %
Charge / e_0	-4	-3,4	-3

FIGURE 2 Chemical structure of deep rough mutant LPS from *E. coli* strain F515, *S. Minnesota* strain R595, and *P. mirabilis* strain R45. Negative charges are indicated by a minus within a black circle, positive charges by a plus within a white circle.

Boggs and Rangaraj, 1985; Peterson et al., 1985) or cathelicidins (Gutsmann et al., 1999, 2000, 2001). Cathelicidins are endogenous peptides, which are in the front line of host defense against invading microorganisms, i.e., Gram-positive and Gram-negative bacteria, mycobacteria, and fungi, by direct physicochemical attack on the surface membranes of these pathogens. Being highly positively charged and amphiphilic, these peptides are perfectly suited to interact with negatively charged membranes, in particular with the LPS leaflet of the OM of Gram-negative bacteria, to cause in a final step disruptive changes in membrane permeability (Gutsmann et al., 2001).

The bioactive part of human cathelicidin hCAP18, an 18 kDa cationic antimicrobial peptide, is a fragment of 37 amino acids (LL37, hCAP18$_{106-142}$) (Larrick et al., 1994). Respective peptides have also been found in various other mammals, such as sheep (SMAP29) (Mahoney et al., 1995) and rabbit (rCAP18) (Larrick et al., 1991). Bioactivity has been found against Gram-negative bacteria such as *E. coli*, *Salmonella enterica* serovar Minnesota and Typhimurium, and Gram-positive bacteria such as *Streptococcus pneumoniae* and *Staphylococcus aureus*. There is, however, no activity of CAP18 against the Gram-negative strain of *Proteus mirabilis*, fungi, and multidrug resistant strains of *Mycobacterium avium* and *Mycobacterium tuberculosis* (Larrick et al., 1993). For the action of various CAP18 fragments, we have established a model of action based on the determination of membrane capacitance, membrane

current, and inner membrane potential difference $\Delta\Phi$ (Gutsmann et al., 2001).

In this article, we establish a setup for the time-resolved determination of the capacitance minimization potential $\Delta\Psi$ on the basis of the IFC method. We determine $\Delta\Psi$ for different asymmetric membranes and compare the results with the respective values of $\Delta\Phi$ determined in ion carrier experiments. Further on, we use this technique to characterize the interaction between different asymmetric bilayers mimicking outer membranes of Gram-negative bacteria and CAP18-derived antibacterial peptides.

MATERIALS AND METHODS

Lipids, peptides, and other chemicals

For the preparation of planar bilayers, Re LPS from *E. coli* strain F515 (LPS F515), *S. Minnesota* strain R595 (LPS R595), and *P. mirabilis* strain R45 (LPS R45) (Zähringer et al., 1985; Rietschel et al., 1992, 1994; Vinogradov et al., 1994; Wiese et al., 1998; Holst, 1999) were used. The chemical structure of the respective LPS is given in Fig. 2. LPS was extracted by the phenol/chloroform/petroleum ether method (Galanos et al., 1969), purified, lyophilized, and transformed into the triethylamine salt form. The amounts of nonstoichiometric substitutions by fatty acids, 4-amino-4-deoxyarabinose (Ara4N), and phosphoethanolamine were analyzed by MALDI-TOF mass spectrometry. Thus, in the LPS R595, the 16:0 fatty acid linked to the amide-linked 3-OH-14:0 in position 2 of the reducing glucosamine was present only at a level of ~30% and Ara4N linked to the 4'-phosphate at a level of 65%. In LPS R45, ~50% of the phosphates linked to the 4'-phosphate of lipid A and 50% of the first Kdo were substituted with Ara4N.

Phosphatidylethanolamine (PE) from *E. coli*, phosphatidylglycerol (PG) from egg yolk lecithin (sodium salt), synthetic diphosphatidylglycerol (DPG), phosphatidylserine (PS) from porcine brain (sodium salt), and synthetic diphytanoylphosphatidylcholine (DPhyPC) were purchased from Avanti Polar Lipids (Alabaster, AL) and used without further purification.

Synthetic CAP18-derived peptides were prepared by Merrifield synthesis as previously described (Larrick et al., 1994) and stored in 0.01% acetic acid. Three fragments of hCAP18 with modified amino acid sequence as compared to the original sequence (m$_1$hCAP18$_{98-117}$, m$_2$hCAP18$_{98-117}$, mhCAP18$_{104-123}$), and three fragments of rCAP18 (rCAP18$_{106-137}$, rCAP18$_{106-125}$, and rCAP18$_{98-117}$) were used (Table 1).

K$^+$-carrier nonactin was obtained from Sigma-Aldrich (Deisenhofen, Germany).

Planar membranes

Planar bilayers according to the Montal-Mueller technique (1972) were prepared as described before (Wiese and Seydel, 1999; Gutsmann et al., 1999). Briefly, asymmetric bilayers were formed by opposing two lipid monolayers each prepared on an aqueous bathing solution from chloroformic solution of the lipids at a small aperture in a thin Teflon septum.

For the formation of planar membranes, phospholipids were dissolved in chloroform (2.5 mg/ml) and LPS in chloroform/methanol (v/v = 10:1) (2.5 mg/ml) by heating to 95°C for 2 min. The PL leaflet of asymmetric LPS/PL membranes consisted of a mixture of PE, PG, and DPG in a molar ratio of 81:17:2 resembling the phospholipid composition of the inner leaflet of the outer membrane of *S. enterica serovar Typhimurium* (Osborn et al., 1972) being composed of the same constituents as that of *E. coli* (Shaw, 1974).

TABLE 1 Amino acid sequences of the six CAP18-derived peptides used in this study

Name	Sequence	Net charge/e_0
$m_1hCAP18_{98-117}$	**DN**_KR_FALL**GD** FF_RK_S_N_E_K_IG—NH$_2$	+2
$m_2hCAP18_{98-117}$	**DN**_KR_FALL_RK_ _R_F_RK_S_N_E_K_IG—NH$_2$	+6
$mhCAP18_{104-123}$	LL**G**DFF_RK_S_N_ E_K_IG_N_E_FK_RI—NH$_2$	+2
$rCAP18_{98-117}$	AQ**E**SP**E**PTGL _RKR_L_RK_F_R_NK—NH$_2$	+5
$rCAP18_{106-125}$	GL_RKR_L_RK_**E**R N_KIK_**E**_K_L_K_- _K_I—NH$_2$	+9
$rCAP18_{106-137}$	GL_RKR_L_RK_**E**R N_KIK_**E**_K_L_K_- _K_I GQ_K_IQGLLP_K_ LA—NH$_2$	+11

Amino acids that are modified as compared to the origin sequence are underlined. Bold characters indicate negative charges, italic characters positive charges. The net charge was calculated under the assumption that K, R, and the N-terminal NH$_2$ are positively charged and E, D, and the C-terminal COOH carry a negative charge.

For electrical measurements, membranes were voltage-clamped via a pair of Ag/AgCl electrodes (type IVM E255, Advanced Laboratory Research, Franklin, MA). All signals were digitized with a PCI-200428W-1 analog input board (Intelligent Instrumentation, Leinfelden-Echterdingen, Germany) and further analyzed by a microcomputer system.

All measurements were performed with bathing solutions consisting of 100 mM KCl and 5 mM MgCl$_2$ at a temperature of 37°C, except for the measurements showing the influence of nonactin on $\Delta\Psi$, where KCl was replaced by NaCl. The bathing solutions were buffered with 5 mM HEPES. Mg^{2+} was used to improve the stability of the membranes. Peptides (100 µg/ml) were added in aliquots of 30 µl to the *cis* side (named first) of the bilayer, e.g., LPS F515/PL.

Capacitance measurements

Membrane capacitance was determined from the first harmonic of the current response to an ac excitation U_1 with a dc bias U_0 according to Carius (1976). To this end, a sine-wave voltage with a frequency ω of 500 Hz and an amplitude of 500 mV$_{rms}$ was applied to the membrane. The capacitive membrane current I_1 was converted into a voltage, low-pass filtered with a four-pole Bessel filter (model 4302, Ithaco, Ithaca, NY) having a cutoff-frequency of 750 Hz, and sent to a microcomputer system. Membrane capacitance C_0 was calculated from the equation

$$I_1 = C_0\left[1 + 3\alpha\left(U_0^2 + \frac{1}{4}U_1^2\right)\right]U_1\omega\cos(\omega t). \qquad (4)$$

We used high-precision capacitors ($\Delta C = \pm\,5$ pF) to calibrate our system.

Inner field compensation

$\Delta\Psi$ was determined by the IFC method according to Sokolov and Kuz'min (1980). The membrane capacitance C_M as a function of the clamp voltage is given by Eq. 3 (Babakov et al., 1966; White, 1970). The current response of a symmetric membrane ($\Delta\Psi = 0$ mV) to an ac excitation with a dc bias $U = U_0 + U_1\sin(\omega t)$ is

$$I(t) = C_0\left[1 + 3\alpha\left(U_0^2 + \frac{1}{4}U_1^2\right)\right]U_1\omega\cos(\omega t)$$
$$+ 3C_0\alpha U_0 U_1^2\omega\sin(2\omega t) - \frac{3}{4}C_0\alpha U_1^3\omega\cos(3\omega t) \qquad (5)$$

(Carius, 1976; Sokolov and Kuz'min, 1980). In the case that $U_0 = 0$ mV, the second harmonic $I_2(t) = 3C_0\alpha U_0 U_1^2\omega\sin(2\omega t)$ vanishes. For an asymmetric membrane ($\Delta\Psi \neq 0$ mV), I_2 vanishes in case that the inner membrane potential difference is compensated by an external voltage (Fig. 3, *B* and *C*).

In our setup, the current response to an ac excitation with a dc bias was analyzed by a lock-in amplifier (7265 DSP lock-in amplifier, EG&G, Berks, UK). The ac excitation with a frequency of 500 Hz and an amplitude of 50 mV$_{rms}$ was generated by the built-in function generator. The dc bias was applied by an analog output board (PCI-200428W-1, Intelligent Instrumentation).

For time-dependent IFC measurements, the dc bias was controlled by a feed-back loop using the phase of the second harmonic as the control parameter. The phase has an inflection point in the case that the inner membrane potential difference $\Delta\Psi$ is compensated by the bias voltage.

Data is stored on the microcomputer system with a frequency of 10 Hz.

Carrier transport measurements

$\Delta\Phi$ was derived from I/U curves obtained from carrier-doped bilayers. For these investigations, the electrodes were connected to the head stage of an L/M-PCA patch-clamp amplifier (List Medical, Darmstadt, Germany). In all cases, the compartment opposite (*trans* compartment) to which the peptide (*cis* compartment) was added, was grounded. Current was defined positive, when cation flux was directed toward the grounded compartment. Membrane current and clamp voltage were low-pass filtered with a four-pole Bessel filter (Ithaco model 4302).

K$^+$-carrier nonactin was added to both compartments before membrane preparation in a final concentration of $\sim$5 × 10^{-7} M, and membranes were
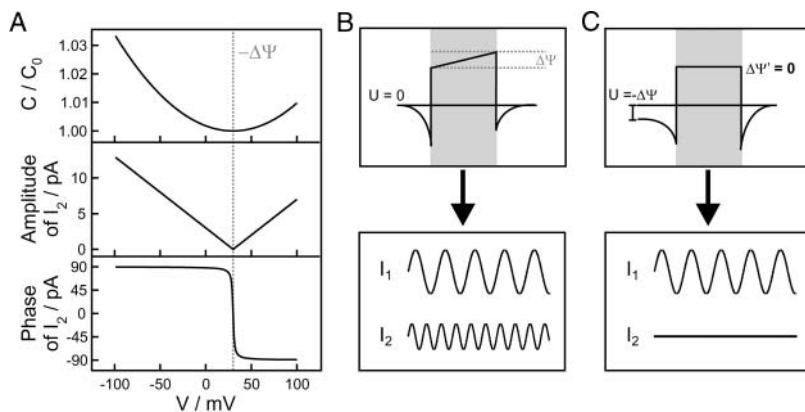
FIGURE 3 Voltage-dependence of the capacitance, amplitude, and phase of the second harmonic (*A*). For inner field compensation measurements, an ac excitation is applied to planar lipid membranes resulting in a current response in the first and the second harmonic ($I_1 \neq 0$, $I_2 \neq 0$) (*B*). When applying an external transmembrane voltage $U = -\Delta\Psi$, the second harmonic vanishes ($I_1 \neq 0$, $I_2 = 0$) (*C*) and the inner membrane potential difference $\Delta\Psi'$ resulting from the inner membrane and the transmembrane potential profile is zero.

prepared as described above. The evaluation of the I/U curves was carried out according to procedures described previously (Seydel et al., 1992). Briefly, the current I as a function of the clamp voltage U is obtained from the Schoch equation

$$I = K \frac{\Delta\Phi + (n_2 - n_1)U}{n_2 - n_1} \frac{\exp(bU) - 1}{\exp(b(\Delta\Phi + n_2 U) - \exp(bn_1 U)},$$

(6)

where $b = (Ze_0)/(kT)$, K is a constant for each membrane, and n_1 and n_2 are the relative distances of the edges of the potential walls for the two leaflets to the membrane surface on the *cis* side.

RESULTS

Determination of the inner membrane potential differences $\Delta\Psi$ and $\Delta\Phi$ of different asymmetric membranes

In Fig. 4, the values of $\Delta\Psi$ and $\Delta\Phi$ for various asymmetric membranes composed of LPS F515, LPS R595, or LPS R45 as well as PS, PG, or DPhyPC on the one and PL on the other side are depicted. $\Delta\Psi$ (*dark gray bars*) was determined by IFC measurements, $\Delta\Phi$ (*light gray bars*) by carrier transport measurements using nonactin-doped membranes. In case of phospholipid/PL membranes, the absolute values for $\Delta\Phi$ and $\Delta\Psi$ differ, but have the same polarity, and with that the inner membrane potential has the same slope, whereas in the case of LPS/PL membranes, $\Delta\Phi$ and $\Delta\Psi$ differ as well in absolute value as in polarity.

To check whether the observed values of $\Delta\Psi$ were determined properly, we induced a defined change of the transmembrane potential by applying a Mg^{2+} concentration gradient across PS/DPhyPC membranes. For a symmetric distribution of Mg^{2+} ions (2 mM on both sides), we observed a value of $\Delta\Psi = 66$ mV. Changing the Mg^{2+} concentration to 10 mM on the PS side led to a reduction of $\Delta\Psi$ by (24 ± 3) mV (data not shown), which is consistent with the expected value of 22 mV according to the Goldman equation.
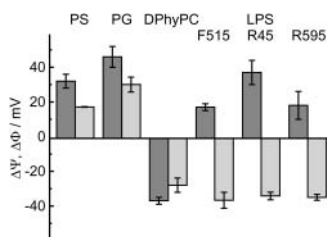

FIGURE 4 Comparison of the inner membrane potential differences $\Delta\Phi$ (*light gray bars*) determined by carrier transport measurements and $\Delta\Psi$ by IFC measurements (*dark gray bars*), respectively, for asymmetric membrane, composed of different phospholipids or lipopolysaccharides. In the figure only one leaflet is defined, the other one was from PL in all cases. The PL side consists of 81 mol % PE, 17 mol % PG, and 2 mol % DPG. Measurements were performed at 37°C in electrolyte solution containing 100 mM KCl and 5 mM $MgCl_2$ buffered with 5 mM HEPES and adjusted to pH 7.

The influence of nonactin on $\Delta\Psi$ of LPS R45/PL membranes was investigated by IFC. It is only possible to determine $\Delta\Psi$ in the absence of a net current, therefore NaCl was used to avoid the transport function of nonactin. The transport rate for Na^+ is reduced by a factor of 1000 as compared to that of K^+. Measurements were performed in electrolyte solution containing 100 mM NaCl and 5 mM $MgCl_2$ buffered with 5 mM HEPES and adjusted to pH 7. After addition of 5 μl, 10 μl, and 30 μl nonactin, no effect on $\Delta\Psi$ could be seen (data not shown).

Change of the inner membrane potential difference $\Delta\Psi$ of various asymmetric membranes after addition of rCAP18_{106–137}

The influence of rCAP18_{106–137} on $\Delta\Psi$ was observed by IFC measurements. rCAP18_{106–137} was added to the *cis* side of various asymmetric membranes composed on one side of PG, DPhyPC, or LPS F515, LPS R595, or LPS R45 and on the other of PL. In Fig. 5, typical potential traces (*black*) are depicted exemplarily for LPS F515/PL (*A*), LPS R45/PL (*B*), and DPhyPC/PL (*C*) membranes. Peptide was added 5 min after membrane preparation (indicated by *arrows*). The gray traces represent relative changes in membrane capacitance C/C_i recorded simultaneously to $\Delta\Psi$. C_i is the initial membrane capacitance determined before peptide addition.

Approximately 60–90 s after addition of 2 μg/ml rCAP18_{106–137} to the LPS side of an LPS F515/PL mem-
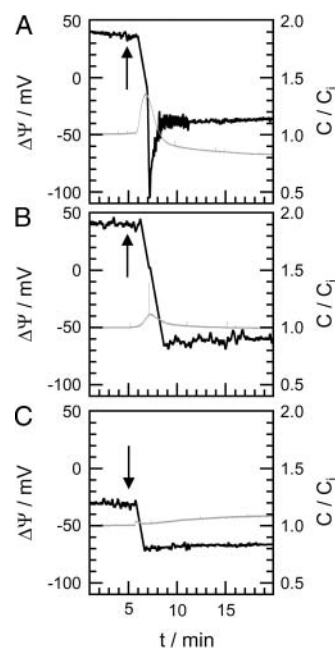

FIGURE 5 Change of the capacitance (*gray traces*) and of the inner membrane potential difference $\Delta\Psi$ (*black traces*) of different membranes after addition of rCAP18_{106–137}. Peptide was added 5 min after membrane preparation (*arrow*): LPS F515/PL (*A*), LPS R45/PL (*B*), and DPhyPC/PL (*C*). Composition of PL side and electrolyte solution as described for Fig. 4.

brane (Fig. 5 A), $\Delta\Psi$ decreases drastically from ~40 mV to −100 mV. A sharp but reduced decrease in $\Delta\Psi$ could also be observed for LPS R45/PL (from 40 mV to –60 mV) and DPhyPC/PL (from −30 mV to −70 mV) membranes (Fig. 5, B and C). Only in the case of LPS F515/PL membranes, $\Delta\Psi$ decreases to a minimal value and increases then to a final value of ~−40 mV. Approximately 5 min after peptide addition, a steady state of $\Delta\Psi$ could be observed for all membranes. In Table 2, the total changes of $\Delta\Psi$ for LPS F515/PL, LPS R595/PL, LPS R45/PL, PG/PL, and DPhyPC/PL membranes, calculated as the sum of the decrease and the increase in $\Delta\Psi$, are given.

Moreover, addition of CAP18 led to changes in membrane capacitance C/C_i. For LPS F515/PL membranes (Fig. 5 A), a sharp increase to ~135% of the initial value and a subsequent drop to ~80% were observed. For LPS R45/PL membranes (Fig. 5 B), a slight increase to ~110% of the initial value followed by a decrease to the initial value occurred. No significant changes were detectable for DPhyPC/PL membranes (Fig. 5 C).

It should be mentioned that both—the changes in $\Delta\Psi$ as well as those in C/C_i—were concentration-dependent. Absolute changes in $\Delta\Psi$ and C/C_i increased with increasing CAP18 concentration (data not shown). In most cases, CAP18 concentrations above 20 μg/ml led to membrane rupture.

Change of the capacitance and the inner membrane potential difference $\Delta\Psi$ of F515 LPS/PL membranes after addition of various CAP18 fragments
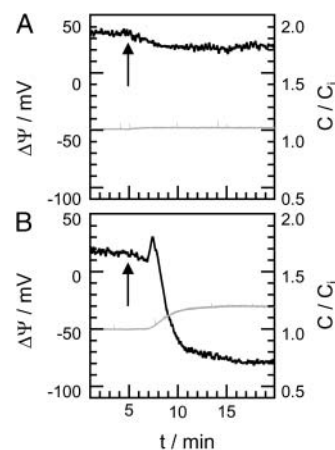
The influence of various CAP18-derived peptides on $\Delta\Psi$ of LPS F515/PL membranes was observed by IFC measurements. Different fragments of CAP18 were added to the *cis* side of asymmetric LPS F515/PL membranes. In Fig. 6, typical potential traces (*black*) are depicted exemplarily for three fragments of rabbit CAP18; the gray traces represent the relative change in membrane capacitance C/C_i. Peptide was added 5 min after membrane preparation (indicated by *arrows*).

Addition of 2 μg/ml rCAP18$_{98-117}$ (Fig. 6 A) to the LPS side of an LPS F515/PL membrane led to a slow decrease in $\Delta\Psi$ from −40 mV to −30 mV. Addition of the same amount of rCAP18$_{106-125}$ (Fig. 6 B) led to a decrease to –80 mV. In

FIGURE 6 Change of the capacitance (*gray traces*) and the inner membrane potential difference $\Delta\Psi$ (*black traces*) of F515 LPS/PL membranes after addition of rCAP18$_{98-117}$ (A) and rCAP18$_{106-125}$ (B). Peptide was added 5 min after membrane preparation (*arrow*). Composition of PL side and electrolyte solution as described for Fig. 4.

comparison to rCAP18$_{106-137}$, the rCAP18$_{106-125}$-induced decrease in $\Delta\Psi$ is not followed by a subsequent increase. In Table 3, the total changes in $\Delta\Psi$ calculated as the sum of the decrease and the increase in $\Delta\Psi$ after addition of 2 μg/ml m$_1$hCAP18$_{98-117}$, m$_2$hCAP18$_{98-117}$, mhCAP18$_{104-123}$, rCAP18$_{98-117}$, rCAP18$_{106-125}$, or rCAP18$_{106-137}$ to the LPS side of an LPS F515/PL membrane are given.

The 20 amino acid-fragment rCAP18$_{98-117}$ (Fig. 6 A) caused no changes in membrane capacitance. After addition of rCAP18$_{106-125}$ (Fig. 6 B), membrane capacitance increases slowly to ~120% of the initial value, which is ~15% less then the change caused by rCAP18$_{106-137}$ (Fig. 5 A). In contrast to the trace recorded after addition of rCAP18$_{106-125}$, rCAP18$_{106-137}$ led to a decrease in capacitance before a steady state was reached.

For all fragments of hCAP18 and rCAP18, a concentration-dependent increase of the absolute changes in $\Delta\Psi$ and C/C_i could be observed (data not shown). At CAP18 concentrations above 20 μg/ml, membrane rupture occurred only for rCAP18$_{106-125}$ and rCAP18$_{106-137}$.

DISCUSSION

Comparison of IFC and carrier transport measurements for the determination of the inner membrane potential difference

In many biological processes, interactions between peptides/ proteins and lipid membranes play an important role. In this report, we investigated the influence of peptides on different electrical properties of reconstituted planar bilayers. To this end, we established a setup for the time-resolved determination of the capacitance minimization potential $\Delta\Psi$ on the basis of the IFC method.

TABLE 2 Total changes in the inner membrane potential difference $\Delta\Psi$ of various asymmetric membranes after addition of rCAP18$_{106-137}$

Lipid matrix	LPS F515/PL	LPS R595/PL	LPS R45/PL	PS/PL	DPhyPC/PL
$\Delta(\Delta\Psi)$/mV	178 ± 14	109 ± 9	123 ± 19	102 ± 3	43 ± 6

Composition of PL side and electrolyte solution as described for Fig. 4. rCAP18$_{106-137}$ was added in aliquots of 2 μg/ml to the *cis* side.

TABLE 3 Total changes in the inner membrane potential difference $\Delta\Psi$ of LPS F515/PL membranes after addition of various CAP18-derived peptides

CAP18	$m_1hCAP18_{98-117}$	$m_2hCAP18_{98-117}$	$mhCAP18_{104-123}$	$rCAP18_{98-117}$	$rCAP18_{106-125}$	$rCAP18_{106-137}$
$\Delta(\Delta\Psi)/mV$	3 ± 8	5 ± 4	4 ± 4	16 ± 4	120 ± 26	178 ± 14

Composition of PL side and electrolyte solution as described for Fig. 4. CAP18 was added in aliquots of 2 μg/ml to the *cis* side.

In our setup, the phase of the second harmonic has been used to control the feedback loop. The phase of the second harmonic has a sharp transition by 180°, and at the same voltage its amplitude drops to 0 pA. Moreover, in contrast to the amplitude, the phase contains information for a directed feedback and with that opens up the possibility to achieve a good time resolution of the apparatus.

In contrast to the determination of $\Delta\Phi$ from carrier-doped membranes, the IFC method yields several advantages, e.g., it does not require any probe molecules (like nonactin or valinomycin) and is not ion-specific. The major advantage of the IFC method is the possibility to perform time-resolved measurements of $\Delta\Psi$, which opens up the possibility to achieve additional information on the timescale of interaction. Furthermore, the IFC allows investigating the influence on $\Delta\Psi$ and C simultaneously.

It should, however, be pointed out that both methods do not allow observing an electrically undisturbed system. In both cases, relatively high voltages as compared to the transmembrane voltage in vivo are applied to the membrane, which might induce reorientation of peptides on the membrane surface and intercalation into the lipid matrix and subsequently the formation of lesions. Furthermore, it should be mentioned that an influence of the ion carrier nonactin on $\Delta\Psi$ in a K^+ free system even at high nonactin concentrations could not be observed.

$\Delta\Psi$ and $\Delta\Phi$ were determined for various asymmetric lipid bilayers. In the focus of our interest was the asymmetric LPS/PL bilayer. LPS (Fig. 2) is the major component of the outer leaflet of the outer membrane of Gram-negative bacteria and is, therefore, a primary target for several antimicrobial peptides such as polymixin B (Wiese et al., 1998), defensins (Sahly et al., 2003), and cathelicidins (Gutsmann et al., 1999). First, we determined the values of $\Delta\Psi$ and $\Delta\Phi$ for several ReLPS/PL and phospholipid/PL membranes and compared the respective values (Fig. 4). Interestingly, a positive linear correlation between $\Delta\Psi$ and $\Delta\Phi$ was only found for phospholipid/PL membranes. Furthermore, $\Delta\Psi$ and $\Delta\Phi$ are linearly correlated with the charge density of the phospholipid leaflet. In contrast to this, we found no correlation between $\Delta\Psi$ and $\Delta\Phi$ in case of LPS/PL membranes.

Interestingly, the values for $\Delta\Psi$ and $\Delta\Phi$ are different for PS/PL and PG/PL membranes. $\Delta\Psi$ differs by a value of 14 mV and $\Delta\Phi$ by 13 mV (Fig. 4). Both lipids, PG and PS, carry one negative net charge, but have a different size (determined from monolayers isotherms). Based on the Gouy-Chapman theory, values of -150 mV and -141 mV were calculated

for the PG and the PS layer, respectively, leading to a difference of 9 mV. Additional contributions to the differences might arise from the Born and the dipole potentials of the two monolayers.

We can only speculate on the overall potential profile of LPS/PL membranes. On the basis of the model from Schoch et al. (1979) (Fig. 7 *A*) for phospholipid membranes we propose a more complex model for LPS/PL bilayers (Fig. 7 *B*) leaving the trapezoidal shape of the overall potential profile and the PL side of the potential profile unchanged. Due to the more complex structure of the LPS headgroup
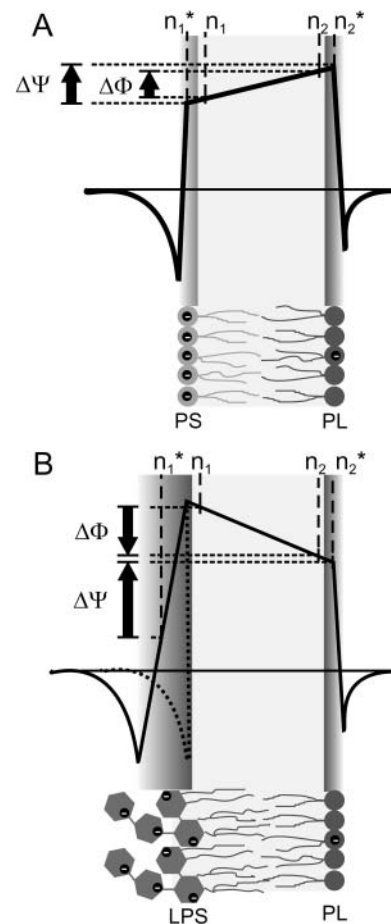
FIGURE 7 Schematic membrane potential profile across asymmetric PS/PL (*A*) and LPS/PL (*B*) membranes on the basis of the Schoch model. The negative charges of the lipid molecules are indicated by black circles. The arrows indicate the polarity of $\Delta\Phi$ and $\Delta\Psi$. The exact potential profile in the headgroups of the LPS molecules is unknown; therefore, we indicated the possible range by a solid line and a dotted line.

(Fig. 2) in comparison to that of phospholipids, in particular its size and the distribution of positive and negative charges in the lipid A portion and the Kdo disaccharide, we expanded the region of the LPS headgroup in the potential profile. The Gouy-Chapman model for the surface potential—based on the assumption that the membrane surface is plane on a molecular scale—could be affected. In the model in Fig. 7 B, we only assumed that the Gouy-Chapman potential is negative and the absolute value is smaller than that of the dipole potential; therefore, the potential increases in the LPS headgroup region from negative to positive values. Due to the lack of knowledge on the exact potential profile in the headgroup region, we used a linear increase as a first approximation.

The carrier nonactin is a molecule with a distinct size, which is smaller than the thickness of phospholipid membranes. Therefore, the carrier transport is influenced mainly by the potential difference between n_1 and n_2 within the hydrophobic region of the bilayers, and the LPS headgroup region has only a minor influence. This is supported by the observation that the three LPS, which differ mainly in their headgroups and not in the hydrophobic part (Fig. 2), have similar values for $\Delta\Phi$ (Fig. 4). In contrast to the carrier transport, the voltage dependence of the capacitance bases on the electromechanical properties (Alvarez and Latorre, 1978) of the entire membrane. Therefore, the potential difference $\Delta\Psi$ might be detected between the positions n_1^* and n_2^* within the membrane. In the case of the phospholipid/PL membranes, the positions n_1 and n_1^* and also n_2 and n_2^* differ only slightly, and subsequently the difference between $\Delta\Phi$ and $\Delta\Psi$ is small (Fig. 7 A). In contrast to this, in the case of LPS/PL membranes, the positions n_1 and n_1^* have to differ significantly with n_1^* located in the LPS headgroup region (Fig. 7 B). This assumption is backed by the results depicted in Fig. 4 showing that $\Delta\Psi$ and $\Delta\Phi$ vary significantly, e.g., they differ in polarity. The two methods, IFC and carrier transport measurements, are complementary and the combination of the results lead to more detailed descriptions of the potential profile.

Characterization of peptide-membrane interaction by IFC

It has been shown earlier that the composition of the lipid matrix of the OM of Gram-negative bacteria plays an important role for the interaction mechanisms with a huge variety of peptides/proteins, membrane proteins (Hagge et al., 2002), as well as antimicrobial peptides (Gutsmann et al., 1999; Wiese et al., 1998). Therefore, we focused on the investigation of interactions of antimicrobial peptides with asymmetric LPS/PL membranes to point out the role of the IFC method for the characterization of peptide-membrane interactions.

First, we performed measurements on the interaction of rCAP18$_{106-137}$ with several lipid bilayers composed on one

side of ReLPS from various sensitive (*E. coli*, *S. Minnesota*) and resistant (*P. mirabilis*) Gram-negative species, as well as several phospholipids and of PL on the other side to study the influence of the lipid matrix. In Fig. 5, typical traces of rCAP18$_{106-137}$-induced changes of $\Delta\Psi$ and C/C_i are depicted.

Applying time-resolved measurements of $\Delta\Psi$ via the IFC technique, we could—for a first time—show that the addition of rCAP18$_{106-137}$ to the LPS side of an LPS F515/PL (Fig. 5 A) membrane mimicking the outer membrane of a sensitive species led to rapid changes in $\Delta\Psi$ as well as in C/C_i indicating a very fast peptide membrane interaction. The interaction process might even be faster because of the still limited sampling rate (~0.1 Hz resulting from the velocity of feedback loop). Furthermore, after starting the IFC measurement, the feedback loop changed the clamp voltage with a maximum speed of ~50 mV/min to finally compensate $\Delta\Psi$, which is about the same rate as the observed peptide-induced changes in $\Delta\Psi$ (Fig. 5). The observed effects were reduced when rCAP18$_{106-137}$ was added to the LPS side of membranes mimicking the outer membrane of a resistant species such as *P. mirabilis* (Fig. 5 B). This observation is in agreement with earlier results showing a reduced capability of the peptide to form lesions in the respective membranes (Gutsmann et al., 1999).

Interestingly, in the case of DPhyPC/PL (Fig. 5 C), rCAP18$_{106-137}$ has only slight influence on the relative membrane capacitance C/C_i whereas $\Delta\Psi$ changed drastically. The latter observation is in contrast to the conclusion published earlier that rCAP18$_{106-137}$ does not interact with PC membranes (Gutsmann et al., 1999, 2000, 2001). These earlier observation were based on the fact that neither the membrane capacitance obtained from planar lipid bilayers nor the film area in monolayer experiments changed significantly. Furthermore, the minimal clamp voltage needed to induce pore formation in DPhyPC/PL membranes is significantly higher as compared to the respective values of LPS/PL membranes. This underlines the role of the IFC method as a very sensitive tool for the investigation of peptide-membrane interactions.

We found that the CAP18-induced changes in $\Delta\Psi$ are linearly correlated with the charge density of the LPS side of the bilayer (Fig. 8), indicating that electrostatic interactions between peptides and membranes play an important role for the accumulation of peptide on the membrane surface and/or the intercalation into the lipid matrix. Similar results for magainin-derived peptides obtained from in vivo studies and liposome assays have been published earlier (Dathe et al., 2001). Interestingly, the results obtained from carrier-doped membranes (Gutsmann et al., 1999) show different final values for $\Delta\Phi$ as compared to $\Delta\Psi$. This is in agreement with the model discussed above that the inner membrane potential differences determined by the two methods are different because of the different positions n_1 and n_1^*.

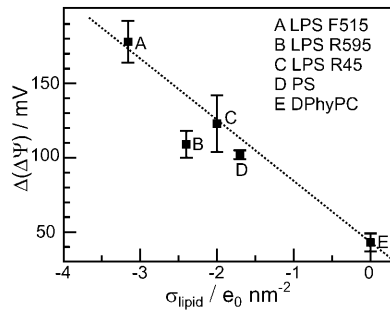Previous studies have shown that several biophysical

FIGURE 8 Correlation between surface charge density σ of the side of peptide addition and change of the inner membrane potential difference $\Delta\Psi$ of various LPS/PL and phospholipid PL membranes. Composition of PL side and electrolyte solution as described for Fig. 4.

parameters modulate activity and selectivity of peptides (Dathe and Wieprecht, 1999; Travis et al., 2000; Pathak et al., 1995). Therefore we studied the influence of several fragments of rabbit and human CAP18—varying in net charge, hydrophobic moment, hydrophobicity, and α-helical content (Gutsmann et al., 2001)—on C/C_i and $\Delta\Psi$ of LPS F515/PL membranes (Figs. 5 A and 6). The results are summarized in Table 3. In Fig. 9, the correlation between net charge and change in $\Delta\Psi$ are given. We found that the change in $\Delta\Psi$ increases with increasing net charge. This also underlines the role of electrostatic interactions in peptide-membrane interactions. This result is in accordance to those found earlier in biological experiments as well as biophysical investigations on different model systems (liposomes, monolayers, planar bilayers) (Gutsmann et al., 2001). Dathe et al. (2001) could show that a modification of charge led to an optimization of the antimicrobial activity of magainin peptides against *E. coli* and *Bacillus subtilis*. These authors found that the antimicrobial activity increases with increasing net charge; however, increase upon a certain threshold led to an increase in hemolytic activity and subsequently a loss of selectivity (Dathe et al., 2001).

Previous studies have shown that asymmetric planar membranes are a powerful method to get a deeper understanding of the interaction mechanisms between peptides/

proteins (polymyxin B, cathelicidins, porins) and bacterial membranes. These studies, however, were limited to the investigation of membrane current, membrane capacitance, and the inner membrane potential $\Delta\Phi$, which does not allow studying the kinetics of the interaction. In this article, we could show that the determination of the inner membrane potential $\Delta\Psi$ by IFC measurements is a helpful and in some cases very sensitive tool for the characterization of properties of lipid bilayers as well as interactions between peptides and membranes and their kinetics. Even though the IFC yields several advantages as compared to the carrier transport measurements, the latter can provide additional information on the system. Therefore, the combination of both methods —IFC and carrier transport measurements—leads to a more detailed description of the interaction mechanism.

REFERENCES

Alvarez, O., and R. Latorre. 1978. Voltage-dependent capacitance in lipid bilayers made from monolayers. *Biophys. J.* 21:1–17.

Babakov, A. V., L. N. Ermishkin, and E. A. Liberman. 1966. Influence of electric field on the capacity of phospholipid membranes. *Nature.* 210:953–955.

Boggs, J. M., and G. Rangaraj. 1985. Phase transitions and fatty acid spin label behavior in interdigitated lipid phases induced by glycerol and polymyxin. *Biochim. Biophys. Acta.* 816:221–233.

Carius, W. 1976. Voltage dependence of bilayer membrane capacitance—-harmonic response to ac excitation with dc bias. *J. Colloid Interface Sci.* 57:301–307.

Cevc, G. 1990. Membrane electrostatics. *Biochim. Biophys. Acta.* 1031:311–382.

Dathe, M., H. Nikolenko, J. Meyer, M. Beyermann, and M. Bienert. 2001. Optimization of the antimicrobial activity of magainin peptides by modification of charge. *FEBS Lett.* 501:146–150.

Dathe, M., and T. Wieprecht. 1999. Structural features of helical antimicrobial peptides: their potential to modulate activity on model membranes and biological cells. *Biochim. Biophys. Acta.* 1462:71–87.

Galanos, C., O. Lüderitz, and O. Westphal. 1969. A new method for the extraction of R lipopolysaccharides. *Eur. J. Biochem.* 9:245–249.

Gutsmann, T., M. Fix, J. W. Larrick, and A. Wiese. 2000. Mechanisms of action of rabbit CAP18 on monolayers and liposomes made from endotoxins or phospholipids. *J. Membr. Biol.* 176:223–236.

Gutsmann, T., S. O. Hagge, J. W. Larrick, U. Seydel, and A. Wiese. 2001. Interaction of CAP18-derived peptides with membranes made from endotoxins or phospholipids. *Biophys. J.* 80:2935–2945.

Gutsmann, T., J. W. Larrick, U. Seydel, and A. Wiese. 1999. Molecular mechanisms of interaction of rabbit CAP18 with outer membranes of Gram-negative bacteria. *Biochemistry.* 38:13643–13653.

Hagge, S. O., H. De Cock, T. Gutsmann, F. Beckers, U. Seydel, and A. Wiese. 2002. Pore formation and function of phosphoporin PhoE of *Escherichia coli* are determined by the core sugar moiety of lipopolysaccharide. *J. Biol. Chem.* 277:34247–34253.
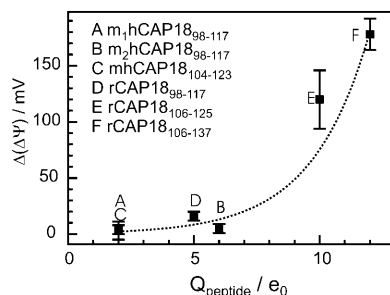

FIGURE 9 Correlation between charge of the peptides Q and change of the inner membrane potential difference $\Delta\Psi$ of LPS F515/PL membranes. Composition of PL side and electrolyte solution as described for Fig. 4.

Holst, O. 1999. Chemical structure of the core region of lipopolysaccharides. *In* Endotoxin in Health and Disease. H. Brade, S. M. Opal, S. N. Vogel, and D. C. Morrison, editors. Marcel Dekker, New York. 115–54.

Kubesch, P., J. Boggs, L. Luciano, G. Maass, and B. Tümmler. 1987. Interaction of polymyxin B nonapeptide with anionic phospholipids. *Biochemistry*. 26:2139–2149.

Larrick, J. W., M. Hirata, Y. Shimomoura, M. Yoshida, H. Zheng, J. Zhong, and S. C. Wright. 1993. Antimicrobial activity of rabbit CAP18-derived peptides. *Antimicrob. Agents Chemother*. 37:2534–2539.

Larrick, J. W., M. Hirata, H. Zheng, J. Zhong, D. Bolin, J.-M. Cavaillon, H. S. Warren, and S. C. Wright. 1994. A novel granulocyte-derived peptide with lipopolysaccharide-neutralizing activity. *J. Immunol*. 152:231–240.

Larrick, J. W., J. G. Morgan, I. Palings, M. Hirata, and M. H. Yen. 1991. Complementary DNA sequence of rabbit CAP18—a unique lipopoly-saccharide binding protein. *Biochem. Biophys. Res. Commun*. 179:170–175.

Lugtenberg, B., and L. Van Alphen. 1983. Molecular architecture and functioning of the outer membrane of *Escherichia coli* and other Gram-negative bacteria. *Biochim. Biophys. Acta*. 737:51–115.

Mahoney, M. M., A. Y. Lee, D. J. Brezinski-Caliguri, and K. M. Huttner. 1995. Molecular analysis of the sheep cathelin family reveals a novel antimicrobial peptide. *FEBS Lett*. 377:519–522.

Montal, M., and P. Mueller. 1972. Formation of bimolecular membranes from lipid monolayers and a study of their electrical properties. *Proc. Natl. Acad. Sci. USA*. 69:3561–3566.

Neumcke, B., and P. Läuger. 1969. Nonlinear electrical effects in lipid bilayer membranes II. Integration of the generalized Nernst-Planck equations. *Biophys. J*. 9:1160–1170.

Osborn, M. J., J. E. Gander, E. Parisi, and J. Carson. 1972. Mechanism and assembly of the outer membrane of *Salmonella typhimurium. J. Biol. Chem*. 247:3962–3972.

Parsegian, V. A. 1975. Ion-membrane interactions as structural forces. *Ann. N. Y. Acad. Sci*. 264:161–171.

Pathak, N., R. Salas-Auvert, G. Ruche, M. H. Janna, D. McCarthy, and R. G. Harrison. 1995. Comparison of the effects of hydrophobicity, amphiphilicity, and alpha-helicity on the activities of antimicrobial peptides. *Proteins*. 22:182–186.

Peterson, A., R. E. W. Hancock, and E. J. McGroarty. 1985. Binding of polycationic antibiotics and polyamines to lipopolysaccharides of *Pseudomonas aeruginosa. J. Bacteriol*. 164:1256–1261.

Pohl, E. E., A. V. Krylov, M. Block, and P. Pohl. 1998. Changes of the membrane potential profile induced by verapamil and propranolol. *Biochim. Biophys. Acta*. 1373:170–178.

Pohl, E. E., U. Peterson, J. Sun, and P. Pohl. 2000. Changes of intrinsic membrane potentials induced by flip-flop of long-chain fatty acids. *Biochemistry*. 39:1834–1839.

Pohl, P., T. I. Rokitskaya, E. E. Pohl, and S. M. Saparov. 1997. Permeation of phloretin across bilayer lipid membranes monitored by dipole potential and microelectrode measurements. *Biochim. Biophys. Acta*. 1323:163–172.

Rietschel, E. T., T. Kirikae, F. U. Schade, U. Mamat, G. Schmidt, H. Loppnow, A. J. Ulmer, U. Zähringer, U. Seydel, F. Di Padova, M.

Schreier, and H. Brade. 1994. Bacterial endotoxin: molecular relationships of structure to activity and function. *FASEB J*. 8:217–225.

Rietschel, E. T., L. Brade, B. Lindner, and U. Zähringer. 1992. Biochemistry of lipopolysaccharides. *In* Bacterial Endotoxic Lipopoly-saccharides, Vol. 1: Molecular Biochemistry and Cellular Biology. D. C. Morrison and J. L. Ryan, editors. CRC Press, Boca Raton, FL. 3–41.

Sahly, H., S. Schubert, J. Harder, P. Rautenberg, U. Ullmann, J. M. Schröder, and R. Podschun. 2003. *Burkholderia* is highly resistant to human Beta-defensin 3. *Antimicrob. Agents Chemother*. 47:1739–1741.

Schindler, P. R. G., and M. Teuber. 1975. Action of polymyxin B on bacterial membranes: Morphological changes in the cytoplasm and in the outer membrane of *Salmonella typhimurium* and *Escherichia coli* B. *Antimicrob. Agents Chemother*. 8:95–104.

Schoch, P., and D. F. Sargent. 1976. Surface potentials of asymmetric lipid bilayers. *Experientia*. 32:811.

Schoch, P., D. F. Sargent, and R. Schwyzer. 1979. Capacitance and conductance as tools for the measurement of asymmetric surface potentials and energy barriers of lipid bilayer membranes. *J. Membr. Biol*. 46:71–89.

Seydel, U., W. Eberstein, G. Schröder, and K. Brandenburg. 1992. Electrostatic potential barrier in asymmetric planar lipopolysaccharide/phospholipid bilayers probed with the valinomycin-K^+ complex. *Z. Naturforsch [C]*. 47:757–761.

Shaw, N. 1974. Lipid composition as a guide to the classification of bacteria. *Adv. Appl. Microbiol*. 17:63–108.

Sokolov, V. S., and V. G. Kuz'min. 1980. Study of surface potential difference in bilayer membranes according to the second harmonic response of capacitance current. *Biofizika*. 25:170–172.

Travis, S. M., N. N. Anderson, W. R. Forsyth, C. Espiritu, B. D. Conway, E. P. Greenberg, P. B. McCray, Jr., R. I. Lehrer, M. J. Welsh, and B. F. Tack. 2000. Bactericidal activity of mammalian cathelicidin-derived peptides. *Infect. Immun*. 68:2748–2755.

Vinogradov, E. V., J. E. Thomas-Oates, H. Brade, and O. Holst. 1994. Structural investigation of the lipopolysaccharide from *Proteus mirabilis* R45 (Re-chemotype). *J. Endotoxin Res*. 1:199–206.

White, S. H. 1970. Thickness changes in lipid bilayer membranes. *Biochim. Biophys. Acta*. 196:354–357.

Wiese, A., M. Münstermann, T. Gutsmann, B. Lindner, K. Kawahara, U. Zähringer, and U. Seydel. 1998. Molecular mechanisms of polymyxin B-membrane interactions: direct correlation between surface charge density and self-promoted uptake. *J. Membr. Biol*. 162:127–138.

Wiese, A., and U. Seydel. 1999. Electrophysiological measurements on reconstituted outer membranes. *Methods Mol. Biol*. 145:355–370.

Zähringer, U., B. Lindner, U. Seydel, E. T. Rietschel, H. Naoki, F. M. Unger, M. Imoto, S. Kusumoto, and T. Shiba. 1985. Structure of de-O-acylated lipopolysaccharide from the *Escherichia coli* Re mutant strain F 515. *Tetrahedron Lett*. 26:6321–6324.

Zheng, C., and G. Vanderkooi. 1992. Molecular origin of the internal dipole potential in lipid bilayers: calculation of the electrostatic potential. *Biophys. J*. 63:935–941.